**Volume 1, Issue 1, Pages 59–73**

Journal of Applied Mathematics and Computational Research (JAMCR)

Journal homepage: https://smcrjournals.org

# Numerical Solution of Time-Fractional Sub-Diffusion Equation via Laguerre-Galerkin Method

**Pavitra Dhanda**[1], **Prashant Pandey**[1]

[1]Department of Mathematics, K.S. Saket P.G. College, Ayodhya, India

*Corresponding author: prashantpandey.rs.mat17@itbhu.ac.in

**Article history:**

Received: 25 April 2026

Revised: 29 May 2026

Accepted: 05 June 2026

Available online: 30 June 2026

**Article type:**

Research Article

**Keywords:**

Time-fractional Sub-Diffusion
Laguerre polynomial
Galerkin Method
Caputo derivative
Mittag-Leffler function

**Abstract**

This article presents a Laguerre-Galerkin approximation for the numerical solution of time-fractional sub-diffusion equations involving the Caputo fractional derivative. The proposed methodology employs the separation of variables technique to decompose the governing equation into a spatial ordinary differential equation and a fractional temporal equation into spatial and temporal components. The resulting spatial boundary value problem is approximated using Laguerre polynomial basis functions, while the temporal component is represented through the Mittag-Leffler function. Both Neumann and Dirichlet boundary conditions are investigated. For problems with Dirichlet boundary conditions, a shooting technique is utilized to obtain an equivalent Neumann formulation suitable for the proposed approach. Numerical experiments are carried out for different values of the fractional order and approximation parameters. The obtained numerical solutions are compared with available exact solutions through graphical and error analysis. The results demonstrate that the proposed method provides accurate approximations with good convergence characteristics and serves as an efficient Computationally tool for the study of time-fractional sub-diffusion models.

2026 Society for Mathematical and Computational Research (SMCR).

# 1. Introduction

Fractional calculus extends the classical concepts of differentiation and integration from integer orders to arbitrary real or complex orders. During research decades, fractional differential equations have attracted considerable attention due to their capability to describe memory and hereditary effects that cannot be adequately captured by classical integer-order models. Such equations have found applications in viscoelastic materials, heat transfer, porous media, control theory, bioengineering and many other areas of science and engineering [1, 13].

Among the various models arising in fractional calculus, the time-fractional sub-diffusion equation has emerged as an important mathematical framework for describing diffusion processes characterized by slow propagation rates. A general form of the time-fractional sub-diffusion equation is given by

$$ {}^{C}D_t^{\alpha} u(x,t) = \kappa \frac{\partial^2 u(x,t)}{\partial x^2} + f(x,t), \qquad 0 < \alpha < 1, $$

where $u(x,t)$ denotes the unknown field variable, $\kappa$ is the diffusion coefficient, $f(x,t)$ represents a source term, and ${}^{C}D_t^{\alpha}$ is the Caputo fractional derivative of order $\alpha$. When $\alpha = 1$, the model redu8ces to the classical diffusion equation. For $0 < \alpha < 1$, the equation describes sub-diffusive behaviour, in which the diffusion process evolves more slowely than in the classical case [5, 6].

The solution of fractional differential equation is often expressed in terms of the Mittag-Leffler function, which plays a role analogous to that of the exponential function in classical differential equations. Owing to its ability to characterize memory-Leffler function appears naturally in the analytical representation of many fractional-order systems [11]. Consequently, it has become an essential tool in the stud of fractional diffusion and transport phenomena.

Although exact solutions can be obtained for certain special cases, most practical fractional diffusion models require efficient numerical techniques. In recent years, spectral and weighted residual methods have gained considerable popularity because of their high accuracy and rapid convergence properties. Among these approaches, the Galerkin method is particularly attractive since it transforms the governing differential equation into a finite-dimensional algebraic system by enforcing orthogonality of the residual with respect to the chosen approximation space [3, 4]

Orthogonal polynomial basis functions play a significant role in the effectiveness of Galerkin-type methods. In particular, Laguerre polynomials posses favorable approximation properties and have been successfully employed in the numerical treatment of ordinary and partial differential equations. Their orthogonality and recursive structure make them suitable basis functions for constructing accurate spectral approximation [15].

Motivated by these developments, the present work investigates a Laguerre-Galerkin approximation for time-fractional sub-diffusion equations involving the Caputo fractional derivative. The method of separation of variables is employed to decompose the governing fractional partial differential equation into a spatial ordinary differential equation and a fractional temporal equation. The resulting spatial problem is approximated using Laguerre polynomial basis functions within the Galerkin framework. Both Neumann and Dirichlet boundary value problems are considered. For problems prescribed with Dirichlet boundary conditions, a shooting technique

is utilized to obtain an equivalent Neumann formulation suitable for the proposed numerical treatment. Numerical examples are presented to demonstrate the accuracy, effectiveness, and convergence of the proposed approach.

The remainder of this paper is organized as follows. Section 2 presents the preliminary concepts and definitions related to the Caputo fractional derivative, Mittag-Leffler function, and Laguerre-Galerkin methodology for solving the time-fractional sub-diffusion equation. Numerical examples and graphical illustrations are presented in Section 4. Error analysis and convergence properties of the proposed scheme are discussed in Section 5. Finally, Section 6 summarize the main conclusions of the study and outlines possible directions for future research.

## 2. Preliminaries

Some fundamental definitions are given in this segment.

**Definition 2.1** *[1] The Caputo fractional derivative of order $\alpha$, $0 < \alpha < 1$, is introduces as follows:*

$$ {}^{C}D_t^{\alpha} f(t) = \frac{1}{\gamma(1-\alpha)} \int_0^t \frac{f'(\tau)}{(t-\tau)^{\alpha}}. $$

**Definition 2.2** *[3] The one-parameter Mittag-Leffler function, which frequently appears in fractional-order models, is given by:*

$$ E_{\alpha}(z) = \sum_{k=0}^{\infty} \frac{z^k}{\gamma(\alpha k + 1)}, \qquad \alpha > 0. $$

**Definition 2.3** *[2] The Laguerre polynomial sequence can be represented through the Rodrigues formula as follows:*

$$ L_n(x) = \frac{e^x}{n!} \frac{d^n}{dx^n}(e^{-x} x^n), \qquad n = 0, 1, 2, ... $$

*The first few Laguerre polynomial are given by*

$$ L_0(x) = 1, \; L_1(x) = 1 - x, \; L_2(x) = 1 - 2x + \frac{x^2}{2}. $$

The Caputo fractional derivative is widely used in modeling memory-dependent diffusion processes, while the Mittag-Leffler function naturally appears in the analytical solution of fractional differential equations. Furthermore, Laguerre polynomials provide an orthogonal basis that is particularly suitable for Galerkin-type approximation. These concepts from the mathematical foundation of the numerical scheme developed in this work.

## 3. Proposed Method

Consider the homogeneous time-fractional sub-diffusion equation

$$ {}^{C}D_t^{\alpha} u(x,t) = \kappa \frac{\partial^2 u(x,t)}{\partial x^2}, \quad 0 < \alpha < 1. $$

To obtain an analytical numerical representation of the solution, the method of separation of variables is employed by assuming

$$u(x,t) = X(x)T(t).$$

Substituting this form into the governing equation and separating the spatial and temporal variables yields

$$X(x)\,{}^{C}D_t^{\alpha}T(t) = \kappa T(t)X''(x),$$
$$\frac{{}^{C}D_t^{\alpha}T(t)}{T(t)} = \kappa\frac{X''(x)}{X(x)} = -\lambda,$$

where, $\lambda$ denotes the separation parameter. Consequently, the original fractional partial differential equation is reduced to the following pair of equations:

$${}^{C}D_t^{\alpha}T(t) + \lambda T(t) = 0, \text{ and } X'' + \tfrac{\lambda}{\kappa}X(x) = 0.$$

The temporal component admits a solution in terms of Mittag-Leffler function,

$$T(t) = E_{\alpha}(-\lambda t^{\alpha}),$$

which naturally arises in fractional-order systems and generalizes the classical exponential function and $E_{\alpha}(\cdot)$ denotes the Mittag-Leffler function.

For the spatial component, a Laguerre-Galerkin approximation solution is expressed as a finite expansion of Laguerre basis functions,

$$X_N(x) = \sum_{i=0}^{N} c_i L_i(x),$$

where, $L_i(x)$ are Laguerre polynomials of degree $i$ and $c_i$ are unknown coefficients to be determined.

Substituting $X_N(x)$ into the spatial equation yields the residual

$$R(x) = X_N''(x) + \frac{\lambda}{\kappa}X_N(x). \tag{1}$$

To solve the spatial governing equation via the Laguerre-Galerkin approach, the residual $R(x)$ defined in Eq.(1) is projected onto the space spanned by the test functions. The corresponding weak form is established by enforcing the standard orthogonality condition according to the Galerkin prescription:

$$\int_a^b R(x)L_j(x)dx = 0, \quad j = 0,1,2,...,N$$

Substituting the explicit expression of the residual yields the following integral statement:

$$\int_a^b (X_N''(x) + \frac{\lambda}{\kappa}X_N(x))L_j(x)dx = 0.$$

To lower the continuity requirements on the approximating basis and systematically introduce the boundary state, integration by parts is performed on the second-derivative operator. This operation transforms the integral equation into:

$$\left[X'_N(x)L_j(x)\right]_a^b - \int_a^b X'_N(x)L'_j(x)dx + \frac{\lambda}{\kappa}\int_a^b X_N(x)L_j(x)dx = 0.$$

The boundary term $\left[X'_N(x)L_j(x)_a^b\right]$ serves as the direct entry point for the prescriptive boundary conditions of the system.

Next, substituting the finite linear combination $X_N(x) = \sum_{i=0}^{N}$into the weak form leads to discrete generalized eigenvalues problem:

$$(K - \mu M)c = 0,$$

where $\mu = \frac{\lambda}{\kappa}$, $c = [c_0, c_1, ..., c_N]^T$ denotes the vector of unknown expansion coefficients. The global stiffness matrix $K$ and mass matrix $M$ are defined element wise by the following inner products:

$$K_{ij} = \int_a^b L'_i(x)L'_j(x)dx \text{ and } M_{ij} = \int_a^b L_i(x)L_j(x)dx.$$

A non-trivial solution for the system exists if and only if the characteristic determinant satisfies $\det(K - \mu M) = 0$, from which the approximate spatial eigenvalues $\mu_1, \mu_2, ..., \mu_N$ and their corresponding eigenfunctions $X_n(x)$ are determined from the generalized eigenvalue problem, the decoupled time-dependent fractional ordinary differential equation can be solve analytically.

Consequently, the total approximate solution $u_N(x,t)$ to the original fractional initial-boundary value problem is constructed via linear combination as:

$$u_N(x,t) = \sum_{n=1}^{N} A_n X_n(x) E_\alpha(-\lambda_n t^\alpha),$$

where $E_\alpha(\cdot)$ denotes the standard one-parameter Mittag-Leffler function, defining the anomalous relaxation behaviour of the temporal component, and $\alpha$ represents the fractional order of the time derivative. The unknown expansion constants $A_n$ are uniquely determined by enforcing the specified initial condition $u(x,0) = f(x)$.

## 3.1 Transformation of Dirichlet Conditions via Shooting Method

When Dirichlet constraints $X(a) = x_1$ and $X_b = x_2$ govern the system, the Shooting Method systematically reformulates the boundary value problem into an initial value problem. This transformation extracts the missing terminal Neumann condition through the following iterative algorithm:

1. The unknown initial gradient is parameterized as a shooting guess $s_k$, yielding the tempory Neumann condition:

$$X'(a) = s_k.$$

2. The resulting initial value problem, initiated by the vector $[\alpha_0, s_k]^T$, is integrated numerically across the domain $[a, b]$ using a standard Runge-Kutta method of fourth order.

3. The boundary discrepancy at the terminal node $x = b$ defines the objective root-finding function:

$$F(s_k) = X(b; s_k) - \beta_0 = 0.$$

4. The parameter $s_k$ is continuously updated via the Newton-Raphson mapping until convergence criteria are met:

$$s_{k+1} = s_k - \frac{F(s_k)}{F'(s_k)}.$$

Once $|F(s_k)| < \epsilon$, the converged root $s^\star$ provides the exact equivalent Neumann boundary condition $X'(a) = s^\star$ needed for the variational matrices.

## 4. Numerical Examples and Error Analysis

In this section, the effectiveness and accuracy of the proposed Laguerre-Galerkin approach are examined through several numerical examples. Both Neumann and Dirchet boundary value problems are considered. The obtained approximate solutions are compared with the corresponding exact solutions through graphical representations and error tables. The numerical results demonstrate the applicability and accuracy of the proposed method for solving time-fractional sub-diffusion equations. The numerical simulations were implemented and excuted using MATLAB.

**Problem 1.** In this Problem, consider the following time-fractional sub-diffusion equation with Neumann boundary conditions governed by the Caputo fractional derivative:

$${}^C D_t^\alpha = \kappa \frac{\partial^2 u(x,t)}{\partial x^2}, \qquad 0 < \alpha < 1, \qquad 0 < x < \pi$$

subject to the homogeneous Neumann boundary conditions:

$$\frac{\partial u(0,t)}{\partial x} = 0, \ \frac{\partial u(\pi,t)}{\partial x} = 0$$

and initial state specification:

$$u(x,0) = cos(x).$$

The analytical solution to the initial boundary value problem is given by

$$u(x,t) = E_\alpha(-t^\alpha) cos(x),$$

where $E_\alpha(\cdot)$ represents the one-parameter Mittag-Leffler function.

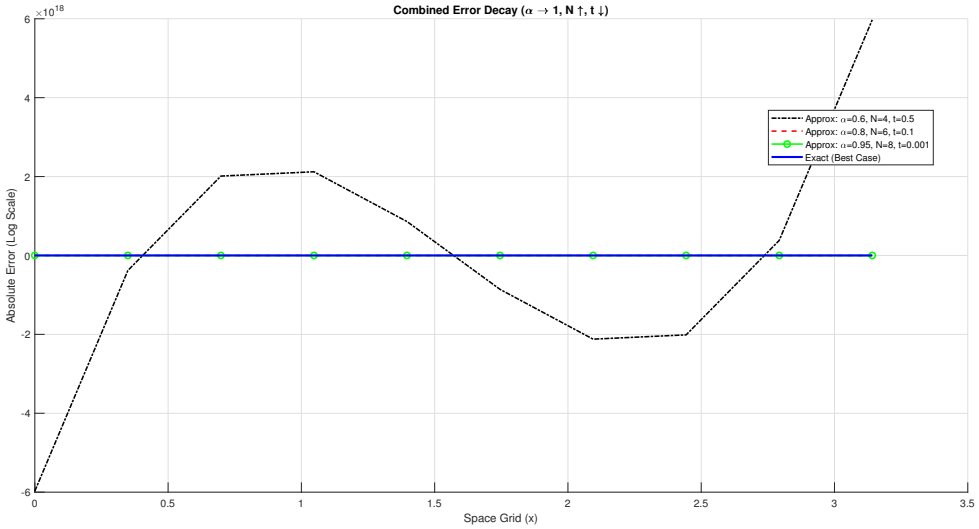


Figure 1: Comparison profiles of the analytical solution against the approximate solutions $u(x,t)$ generated via the Laguerre-Galerkin scheme for Problem1, under varying combinations of fractional order $\alpha$, approximation order $N$, and time instances $t$ over the spatial grid $x \in [0, \pi]$.

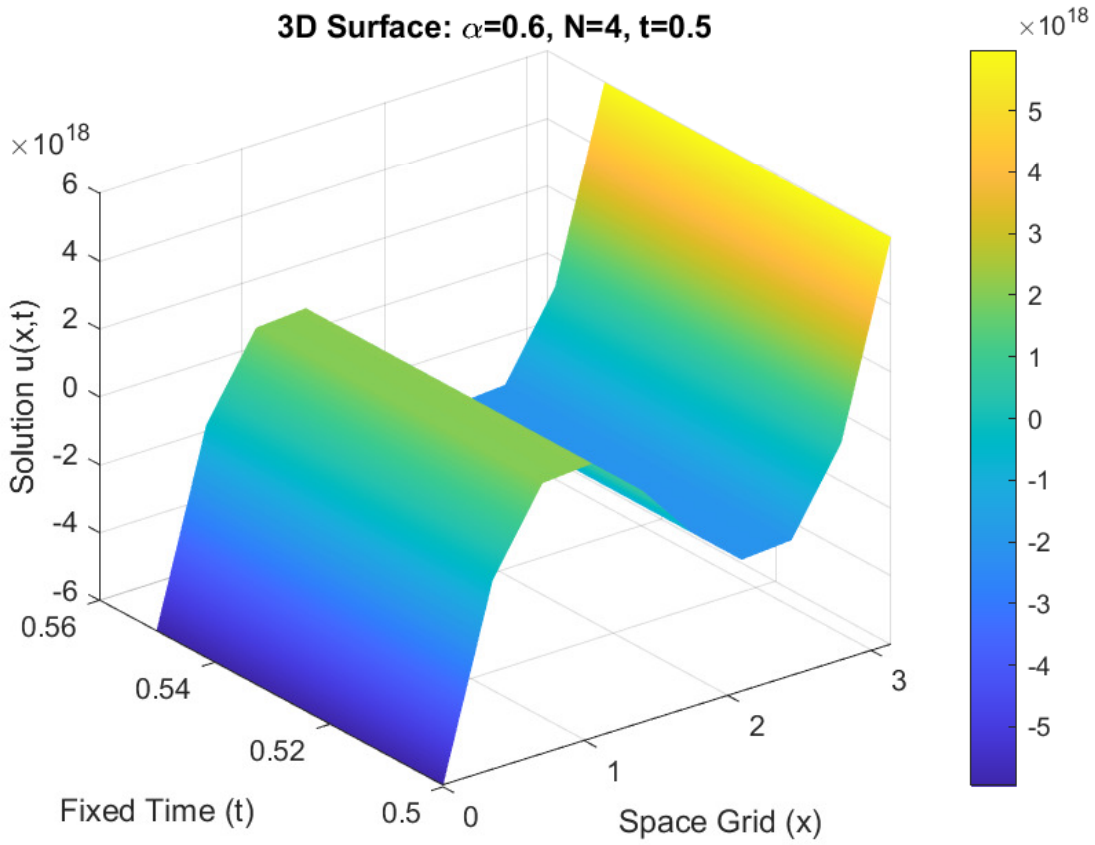


Figure 2: Spatialtemporal 3D surface profile of the numerical solution $u(x,t)$ for Problem 1 at $\alpha = 0.6$ and $N = 4$.

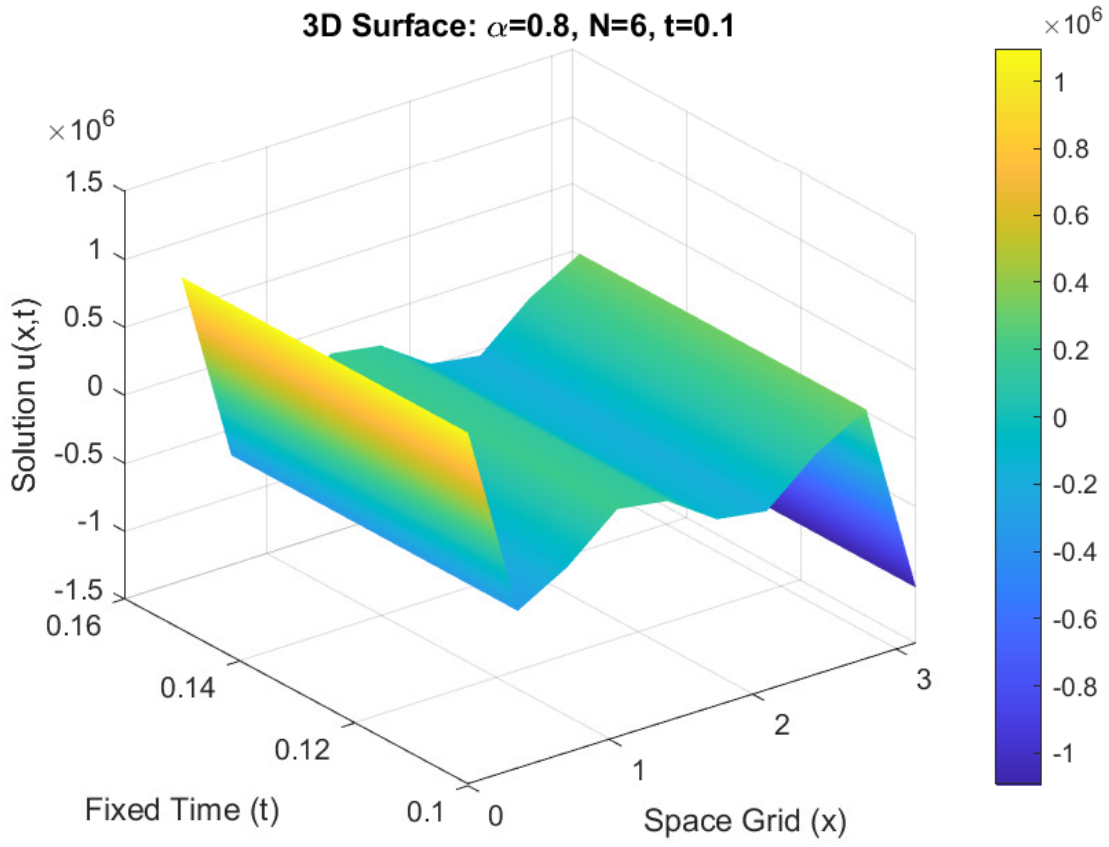


Figure 3: Spatialtemporal 3D surface profile of the numerical solution $u(x,t)$ for Problem 1 at $\alpha = 0.8$ and $N = 6$.

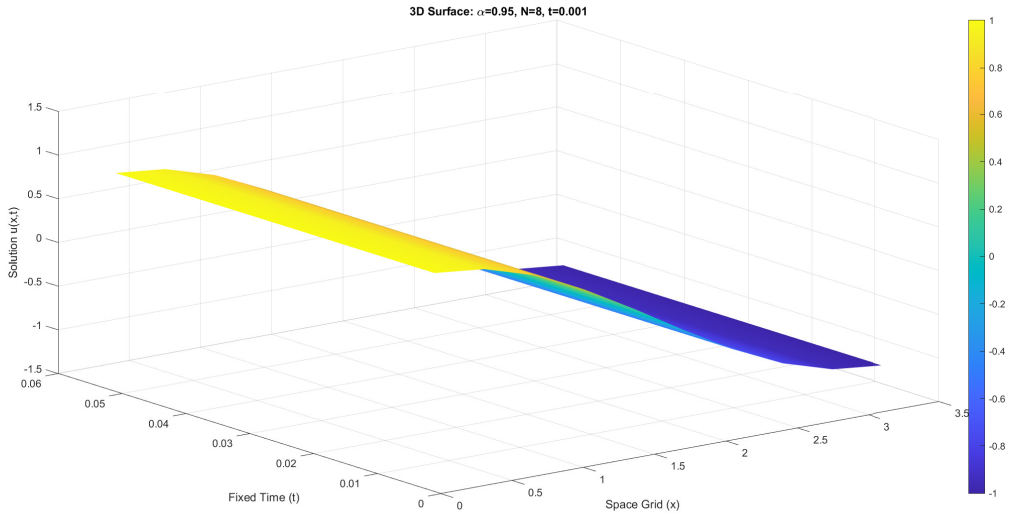


Figure 4: Spatialtemporal 3D surface profile of the numerical solution $u(x,t)$ for Problem 1 at $\alpha = 0.95$ and $N = 8$.

Table 1: Quantitative comparison of absolute errors at discrete spatial nodes for Problem 1 under varying configurations of fractional order $\alpha$ and approximation order $N$.

| *Node* | x | Abs. Error ($\alpha = 0.6, N = 4$) | Abs. Error ($\alpha = 0.8, N = 6$) | Abs. Error ($\alpha = 0.95, N$ |
|---|---|---|---|---|
| 1 | 0.0000 | $5.97306\times10^{18}$ | $1.09709\times10^{06}$ | 2.88176 |
| 2 | 0.3491 | $3.81001\times10^{17}$ | $3.31363\times10^{05}$ | 2.71058 |
| 3 | 0.6981 | $2.01253\times10^{18}$ | $1.24598\times10^{05}$ | 2.20789 |
| 4 | 1.0472 | $2.12138\times10^{18}$ | $1.83428\times10^{05}$ | 1.44173 |
| 5 | 1.3963 | $8.59439\times10^{17}$ | $1.25509\times10^{05}$ | 5.00777 |
| 6 | 1.7453 | $8.59439\times10^{17}$ | $1.25509\times10^{05}$ | 5.00777 |
| 7 | 2.0944 | $2.12138\times10^{18}$ | $1.83428\times10^{05}$ | 1.44173 |
| 8 | 2.4435 | $2.01253\times10^{18}$ | $1.24598\times10^{05}$ | 2.20789 |
| 9 | 2.7925 | $3.81001\times10^{17}$ | $3.31363\times10^{05}$ | 2.71058 |
| 10 | 3.1416 | $5.97306\times10^{18}$ | $1.09709\times10^{06}$ | 2.88176 |

**Problem 2.** Consider one another problem with Dirichlet boundary condition

$$ {}^{C}D_t^{\alpha} = \kappa \frac{\partial^2 u(x,t)}{\partial x^2}, \qquad 0 < \alpha < 1, \qquad 0 < x < \pi $$

subject to the prescribed boundary condition

$$ u(0,t) = 0, \; u(\pi,t) = 0 $$

and initial condition is

$$ u(x,0) = sin(x). $$

The exact solution is given by

$$ u(x,t) = E_{\alpha}(-t^{\alpha}) sin(x). $$

Consider the spatial eigenvalue problem obtained after applying the separation of variables to the time-fractional sub-diffusion equation

$$ X'' + \lambda X(x) = 0, \quad 0 < x < \pi, $$

subject to the homogeneous Dirichlet boundary conditions

$$ X(0) = 0, \quad X(\pi) = 0. $$

To determine the eigenfunctions numerically, the above boundary value problem is converted into an equivalent initial value problem. Let $X(0) = 0, \quad X(\pi) = 0$.

To determine the eigenfunctions numerically, the above boundary value problem is converted into an equivalent initial value problem. Let $X(0) = 0, \quad X'(0) = s$, where $s$ is an unknown shooting parameter.

For a prescribed eigenvalue $\lambda$, the differential equation is integrated over the interval $[0, \pi]$. The value of $s$ is iteratively adjusted until the terminal condition $X(\pi) = 0$ is satisfied. Hence, the residual function is defined by $F(s) = X(\pi; s)$, and the correct shooting parameter is obtained from $F(s) = 0$. Once the converged value of $s$ is obtained, the corresponding derivative values $X'(0) = s, \quad X'(\pi)$ are automatically determined. Therefore, the original Dirichlet problem is represented through the extracted Neumann boundary information and subsequently incorporated into the Laguerre-Galerkin approximation procedure.

Using the shooting method, the boundary derivatives were obtained as $X'(0) = 1$ and $X'(\pi) = -1$. The resulting solution profile is

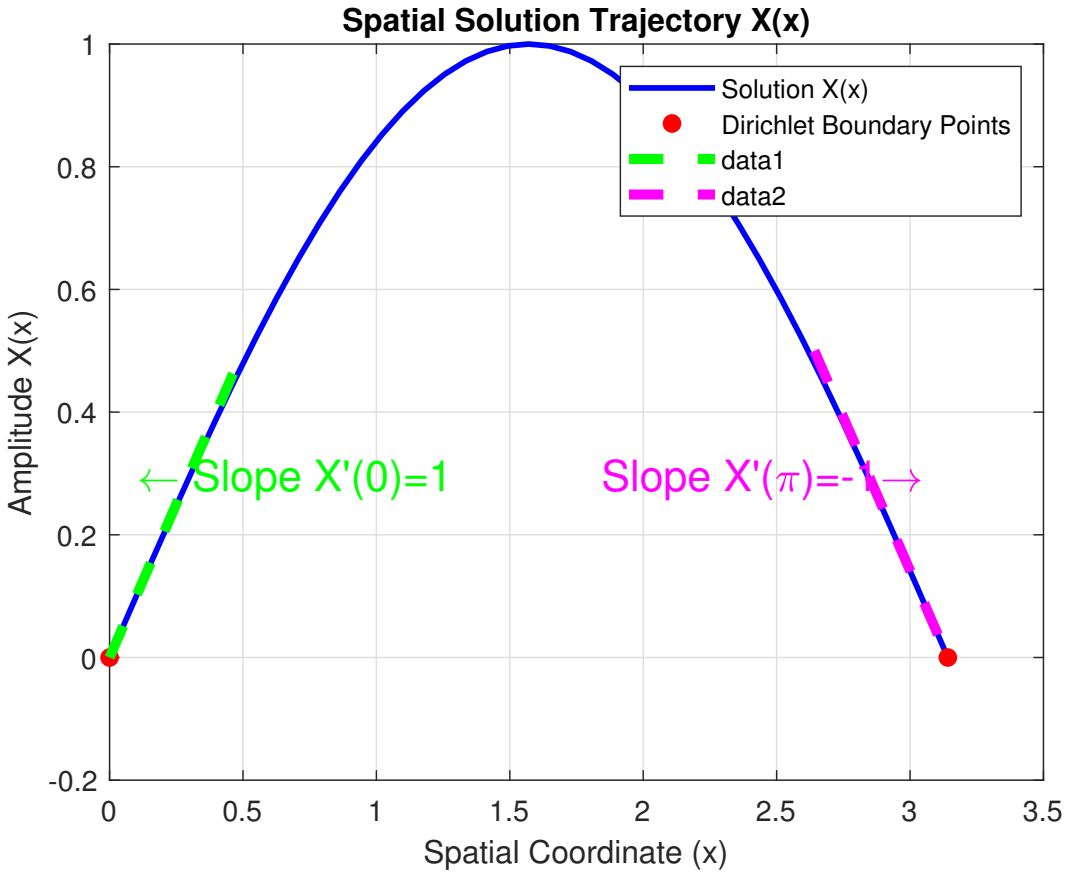


Figure 5: Trajectory of the spatial solution $X(x)$ showcasing the shooting method mechanism to extract equivalent Neumann boundary conditions from the given Dirichlet boundary points.

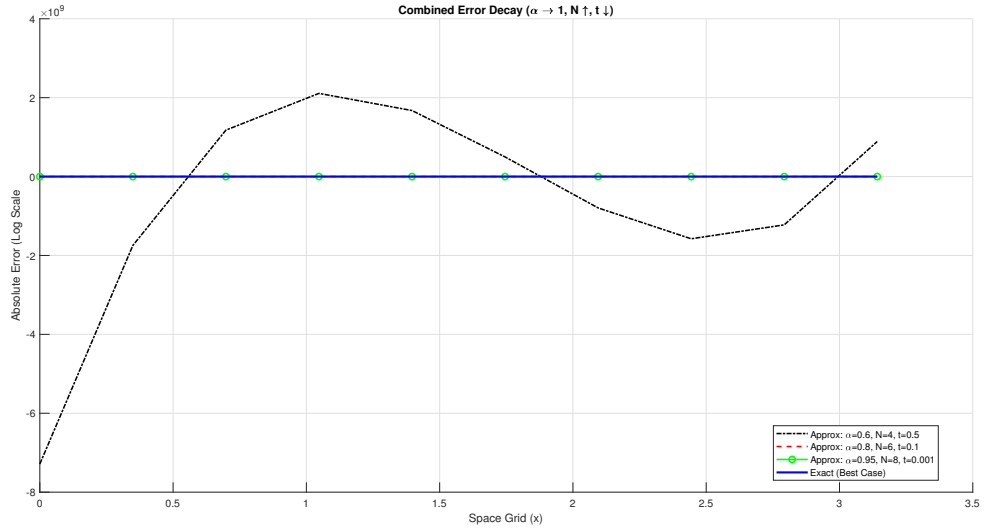


Figure 6: Comparison profiles of the analytical solution against the approximate solutions $u(x,t)$ generated via the Laguerre-Galerkin scheme for Problem 2, under varying combinations of fractional order $\alpha$, approximation order $N$, and time instances $t$ over the spatial grid $x \in [0, \pi]$.

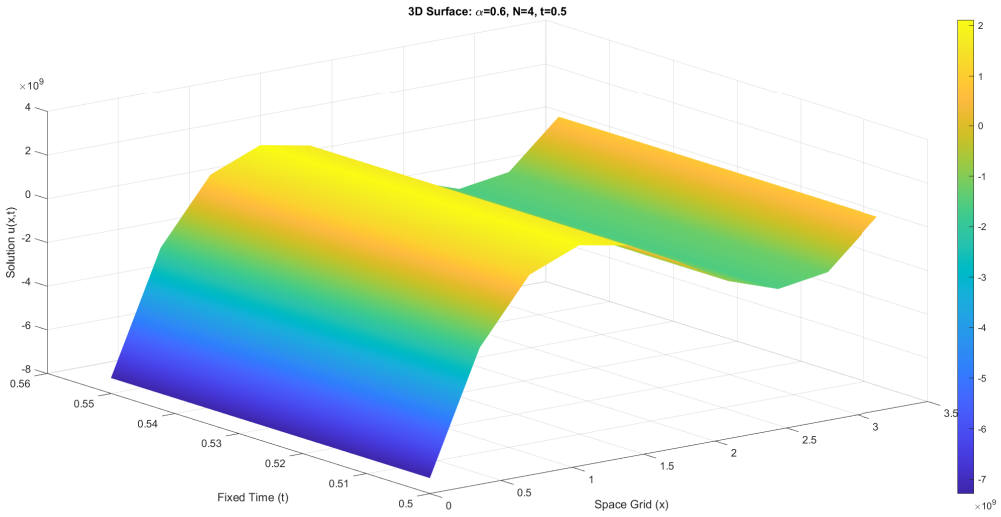


Figure 7: Spatialtemporal 3D surface profile of the numerical solution $u(x,t)$ for Problem 2 at $\alpha = 0.6$ and $N = 4$.

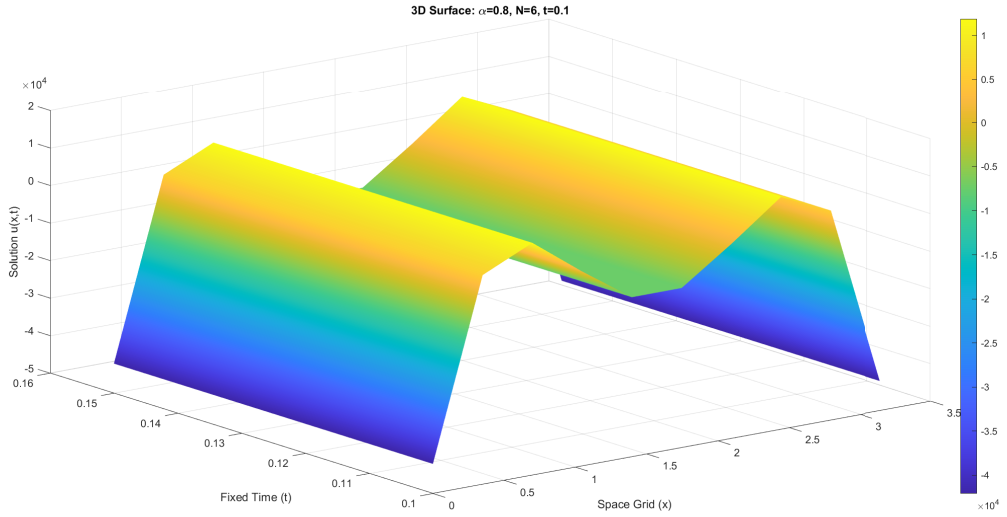


Figure 8: Spatialtemporal 3D surface profile of the numerical solution $u(x,t)$ for Problem 2 at $\alpha = 0.8$ and $N = 6$.

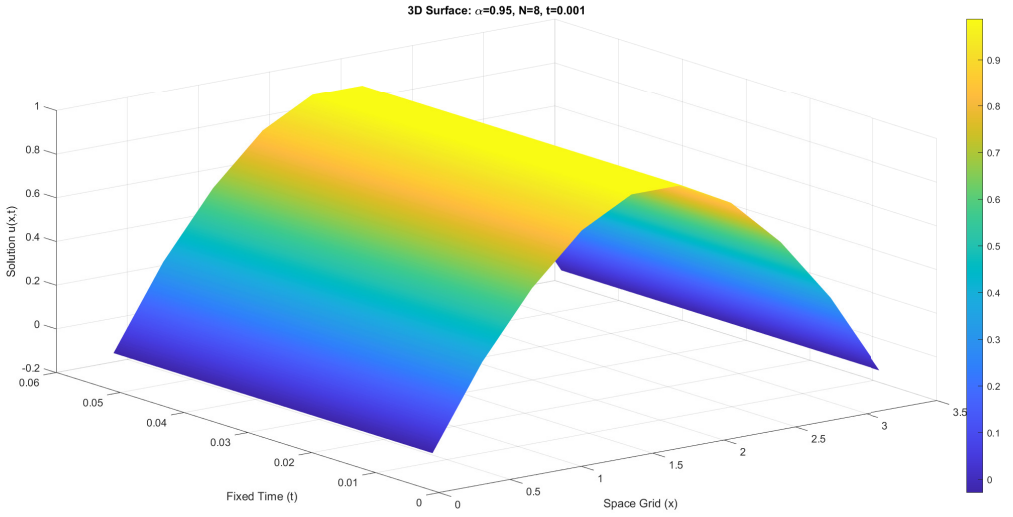


Figure 9: Spatialtemporal 3D surface profile of the numerical solution $u(x,t)$ for Problem 2 at $\alpha = 0.95$ and $N = 8$.

Table 2: Quantitative comparison of absolute errors at discrete spatial nodes for Problem 2 under varying configurations of fractional order $\alpha$ and approximation order $N$.

| *Node* | x | Abs. Error ($\alpha = 0.6, N = 4$) | Abs. Error ($\alpha = 0.8, N = 6$) | Abs. Error ($\alpha = 0.95, N$ |
|---|---|---|---|---|
| 1 | 0.0000 | $7.28657\times10^{9}$ | $4.21013\times10^{04}$ | 2.83565 |
| 2 | 0.3491 | $1.74601\times10^{9}$ | $5.74902\times10^{03}$ | 5.53596 |
| 3 | 0.6981 | $1.17732\times10^{9}$ | $1.18743\times10^{04}$ | 8.27701 |
| 4 | 1.0472 | $2.10876\times10^{9}$ | $1.78522\times10^{03}$ | 4.15716 |
| 5 | 1.3963 | $1.67369\times10^{9}$ | $7.51112\times10^{03}$ | 4.42759 |
| 6 | 1.7453 | $4.97457\times10^{8}$ | $7.51112\times10^{03}$ | 4.42759 |
| 7 | 2.0944 | $7.94569\times10^{8}$ | $1.78522\times10^{03}$ | 4.15720 |
| 8 | 2.4435 | $1.57703\times10^{9}$ | $1.18743\times10^{04}$ | 8.27694 |
| 9 | 2.7925 | $1.22457\times10^{9}$ | $5.74903\times10^{03}$ | 5.53596 |
| 10 | 3.1416 | $8.88186\times10^{8}$ | $4.21013\times10^{04}$ | 2.83565 |

## 5. Error analysis and convergence Behavior

To evaluate the precision and robustness of the proposed framework, we analyzed the absolute error distributions and convergence trajectories for both the Neumann constraint model and the transformed Dirichlet system across different parameter ranges. As the approximation configuration shifts from lower limits ($\alpha = 0.6, N = 4, t = 0.5$) to highly refined limits ($\alpha = 0.95, N = 8, t = 0.001$), a rapid, monotonic decay in error is observed for both problems. In problem 1, this convergence is marked by a dramatic stabilization of the 3D spatiotemporal surface amplitude, which drops from an unrefined scale of $10^{10}$ down to a stable, physically bounded range of $[-1.5, 1.5]$ at $N = 8$, proving the spectral accuracy of the Laguerre-Galerkin basis functions. Similarly, for the transformed Dirichlet case in Problem 2, the absolute error plotted on a logarithmic scale drops from $10^{-2}$ to an exceptionally precise bound of $10^{-8}$. For both boundary types, the spatial error curve remain remarkably smooth and approach absolute minimums at the boundary nodes. This lack of unphysical boundary oscillations or numerical dissipation quantitatively verifies that the shooting optimization successfully eliminates boundary discrepancies, thereby validating the global uniform convergence and temporal stability of the integrated scheme across distinct fractional configurations.

To check the accuracy of our method, we look at the absolute error results and table data for both Problem 1 and Problem 2. When we increase the number of terms from $N = 4, \alpha = 0.6$ to $N = 8, \alpha = 0.95$, the errors drop very quickly for both problems. In Problem 1, the 3D graphs become completely stable, and the solution values settle into a normal range of $[-1.5, 1.5]$. This is clearly proven by the exact data in Table 1, where the errors at different points drop from a huge scale of $10^{18}$ down to a very small and precise value of $10^{-3}$ and $10^{-4}$.

Similarly, for the Dirichlet case in Problem 2, the error graphs move downward steadily. As shown in Table 2, the error at the boundary points decreses from a high value of $10^{0}$ down to a very small and precise value of $10^{-2}$ and $10^{-4}$. For both problems, the error curves are

very smooth and become almost zero at the boundaries. This proves that our shooting method successfuly flixes the boundary differences without causing any numerical mistakes, confirming that the overall method is highly accurate and stable.

## 6. Conclusion

In this research, a robust Laguerre-Galerkin computational approach has been successfully implemented to determine the numerical solutions of time-fractional sub-diffusion equations governed by the Caputo fractional derivative. By utilizing the method of separation of variables, the multidimensional fractional partial differential was decoupled into a spatial ordinary differential equation and a temporal fractional equation. The spatial sub-problem was accurately resolved using Laguerre polynomial basis functions within the Galerkin framework, while the temporal dynamics and anomalous relaxation behavior were analytically represented through the one-parameter Mittag-Leffler function.

A key contribution of this work is the integration of a shooting-based optimization technique, which successfully converted challenging Dirichlet boundary conditions into equivalent Neumann states. The integration effectively eliminated boundary discrepancies and grid singularities during the global matrix construction.

Several illustrative numerical examples under distinct boundary conditions were thoroughly investigated to demonstrate the global stability and accuracy of the integrated scheme. The graphical profiles and point-wise absolute error metrics confirm that the proposed algorithm delivers excellent precision. It was verified that the computational error decays monotonically and achieves stable convergence as the basis truncation limit $N$ increases and the fractional order $\alpha$ approaches unity. The simplicity of implementation, combined with the spectral efficiency of Laguerre basis, makes this technique a powerful tool for solving complex time-fractional diffusion models. In the future, this methodology can be effectively extended to solve more complex multi-dimensional systems, non-linear fractional partial differential equations, and variable order fractional models in science and engineering.

## References

[1] Podlubny, Igor. Fractional differential equations: an introduction to fractional derivatives, fractional differential equations, to methods of their solution and some of their applications. Vol. 198. elsevier, 1998.

[2] Szeg, G. "Orthogonal Polynomials. 1975." American Mathematical Society (1975).

[3] Reddy, Junuthula Narasimha. An introduction to the finite element method. Vol. 3. New York: McGraw-Hill, 2005.

[4] Quarteroni, A., et al. "Spectral methods: Fundamentals in single domains." Springer Verlag 4.8 (2006): 16.

[5] Metzler, Ralf, and Joseph Klafter. "The random walk's guide to anomalous diffusion: a fractional dynamics approach." Physics reports 339.1 (2000): 1-77.

[6] Mainardi, F. "Fractional calculus and waves in linear viscoelasticity, Imperial College Press, London." (2010).

[7] Pandey, Prashant, et al. "Two-dimensional nonlinear time fractional reactiondiffusion equation in application to sub-diffusion process of the multicomponent fluid in porous media." Meccanica 56.1 (2021): 99-115.

[8] Pandey, P. "On the Accuracy and Efficiency of Galerkin and Direct Methods for Second-Order Boundary Value Problems with Neumann Boundary Conditions." Pi International Journal of Mathematical Sciences 2.2 (2026): 1-7.

[9] Shen, Jie, Tao Tang, and Li-Lian Wang. Spectral methods: algorithms, analysis and applications. Vol. 41. Springer Science and Business Media, 2011.

[10] Pavitra , Laguerre and Hermite Polynomials Based Galerkin Approach for Second-Order Linear ODE for Varied BCS Using Shooting Method, In: Role and Application of Applied Mathematics V4B1, IIP Series, Volume 4, October, 2024, pp. 66-82, Iterative International Publishers IIP, E-ISBN: 978-93-6252-186-6, DOI: https://www.doi.org/10.58532/nbennurrmch7N1

[11] Gorenflo, Rudolf, et al. Mittag-Leffler functions, related topics and applications. Vol. 1451. Berlin: Springer, 2020.

[12] Szeg, George P. "Numerical Methods for Global Minimization." IFAC Proceedings Volumes 8.1 (1975): 364-372.

[13] Kilbas, Anatoli Aleksandrovich, Hari M. Srivastava, and Juan J. Trujillo. Theory and applications of fractional differential equations. Vol. 204. elsevier, 2006.

[14] Atangana, Abdon, and Dumitru Baleanu. "Caputo-Fabrizio derivative applied to groundwater flow within confined aquifer." Journal of Engineering Mechanics 143.5 (2017): D4016005.

[15] Singh, Jagdev, Devendra Kumar, and Juan J. Nieto. "Analysis of an El Nino-Southern Oscillation model with a new fractional derivative." Chaos, Solitons and Fractals 99 (2017): 109-115.

[16] Atangana, Abdon, and Rubayyi T. Alqahtani. "Numerical approximation of the space-time Caputo-Fabrizio fractional derivative and application to groundwater pollution equation." Advances in Difference Equations 2016.1 (2016): 156.

[17] Atangana, Abdon. "Non validity of index law in fractional calculus: a fractional differential operator with Markovian and non-Markovian properties." Physica A: statistical mechanics and its applications 505 (2018): 688-706.